

Received September 15, 2019, accepted October 11, 2019, date of publication October 15, 2019, date of current version October 25, 2019.

Digital Object Identifier 10.1109/ACCESS.2019.2947601

# Color Image Invariant Feature Extraction by a Topological Property Motivated PCNN Model

GUANGJIE KOU<sup>1</sup>, JUN YUE<sup>1</sup>, YUNYAN MA<sup>2</sup>, AND ZHIWANG ZHANG<sup>1</sup>

<sup>1</sup>School of Information and Electrical Engineering, Ludong University, Yantai 264025, China

<sup>2</sup>School of Mathematics and Statistics, Ludong University, Yantai 264025, China

Corresponding author: Guangjie Kou (kouguangjie@126.com)

This work was supported in part by the Natural Science Foundation of Shandong Province under Grant ZR2017MF062, Grant ZR2017MF010, and Grant ZR2017MF035, and in part by the National Natural Science Foundation of China under Grant 61472172, Grant 61100115, Grant 61877061, and Grant 61771231.

**ABSTRACT** Topological invariant features take priority over other vision features in early visual perception stage, which is the core idea of topological perception theory. In order to improve the robustness and distinguishability of the invariant features extracted by pulse coupled neural network (PCNN), the topological properties are integrated into PCNN. The improved PCNN model is called as topological property motivated PCNN (TPCNN), which adopts the saliency map calculated by the spectral residual approach as the important topological properties (the connectivity, and the number of holes in target). In TPCNN, firstly, the normalized saliency map is used as a linking coefficient to enhance the importance of saliency object when we calculating the invariant features. Secondly, the entropy signature of the saliency map is treated as an additional new feature and merged into original features calculated by PCNN, then the final invariant feature is obtained. The proposed TPCNN is used to calculate the invariant feature of different kinds of fish in the paper. Experimental results show that TPCNN outperforms the state-of-art models on invariant features extraction.

**INDEX TERMS** Pulse coupled neural network, invariant feature extraction, topological perception theory, saliency map, spectral residual approach.

## I. INTRODUCTION

As a bio-inspired neural network model, the pulse coupled neural network (PCNN) [1], [2] has many good characteristics, such as a single layer, no prior training is required, possessing a good theoretical basis of the biological vision system, etc. Nowadays, PCNN is widely used in image segmentation [3]–[5], image enhancement [6], image authentication [7], [8], image fusion [9], feature extraction and pattern recognition [10]–[14] etc. Though it already has a good performance about the invariant features (also called image signature) extracted by basic PCNN, great changes may happen when the target's shaping changes a little. To improve the robustness and distinguishability of the invariant features calculated by basic PCNN. We reference the topological perception theory [15], [16] of cognitive psychology and introduce the topological property into the simplified PCNN model. A topological property motivated PCNN (TPCNN) is

The associate editor coordinating the review of this manuscript and approving it for publication was Haiyong Zheng <sup>1</sup>.

proposed and it is used to extract the color image invariant features successfully in the paper.

Topological perception theory [15], [16] is an important branch of cognitive psychology. It is the psychological foundation of TPCNN model. The core idea of Topological perception theory is that visual perception organization should be interpreted as transformation and invariance over transformation. In this procedure, topological properties are more stable (global) than other local geometrical properties. The perception of topological properties is earlier than the perception of local geometrical properties in the vision process. These inspire us to introduce topological properties into the classical PCNN. Topological properties used in this paper are calculated by the spectral residual method [17]. We use the saliency map [18], [19] computed by a spectral residual approach to express the important topological properties: connectivity and number of holes in the objects. The robustness and distinguishability of the invariant features calculated by TPCNN are improved significantly than other ordinary models such as classical PCNN [1], [2], SCM [11], SPCNN [12], FLM [6], [14], etc.

The structure of this paper is divided into seven sections. Section II briefly introduces the topological perception theory and the spectral residual approach. The relationship between topological properties and the saliency map are discussed. Section III presents and analyzes our topological property motivated PCNN model (TPCNN) in detail. Section IV gives the detailed procedure of color image invariant feature extraction method based on TPCNN. In Section V, the robustness and effectiveness of the TPCNN signature are proved by a large number of experimental results. Section VI introduces several typical applications of the TPCNN signature. The conclusion is given in Section VII.

## II. TOPOLOGICAL PERCEPTION THEORY AND SPECTRAL RESIDUAL APPROACH

### A. TOPOLOGICAL PERCEPTION THEORY

Topological perception theory is proposed by Chen [15] in 1982. It's an important branch of cognitive psychology. The theory includes one core idea and two main aspects. The core idea is that visual perception organization should be interpreted as transformation and invariance over transformation. The first aspect emphasizes that the topological structure is the most stable and invariant during vision perception forming. The second aspect highlights the topological perception is prior and sensitive to the perception of local vision features (local geometrical properties).

To explain the visual perception organizational process, a *global-to-local* model is proposed in topological perception theory. The order of global to local reflects the descending order of vision properties' stability. A vision property is considered more stable (or global) if it remains invariant under a more general transformation. Topological transformation is more general relative to geometrical transformation. Thus, the topological properties are more stable (global) than other vision features. The more stable a property is, the earlier it is perceived in early visual perception stage. The topological properties are also called topological invariant features, such as the connectivity, the relationship of inside and outside, and the number of holes in the target. These topological properties maintained good invariant feature when the object over topological (shape-changing) transformations. For example, the topological properties of a dog keep invariant, whether it is standing or lying. However, the geometrical properties are different for a standing dog and lying dog.

In summary, the stability of invariant features calculated by the improve PCNN can be improved significantly, if we introducing topological properties into the classical PCNN.

### B. SPECTRAL RESIDUAL APPROACH

Different from other saliency detection algorithms [18], [19], spectral residual approach [17] is a general algorithmic framework and independent of the objects' prior knowledge, such as color, texture, etc. By calculating the spectral residual of an input image in the spectral domain, it can construct the saliency map in spatial domain fastly. Therefore, this method

is very suitable to extract the salient object's silhouette. As the connectivity and the number of holes (two important topological properties) are contained in object's silhouette, the saliency map constructed by spectral residual approach is used to express the topological properties in the following sections.

The spectral residual approach can be expressed as following five equations [17].

$$A(f) = \text{amplitude}(F[I(i, j)]) \quad (1)$$

$$P(f) = \text{phase}(F[I(i, j)]) \quad (2)$$

$$L(f) = \log(A(f)) \quad (3)$$

$$R(f) = L(f) - h_n(f) * L(f) \quad (4)$$

$$S(i, j) = g(i, j) * F^{-1} - [\exp(R(f) + P(f))]^2 \quad (5)$$

where  $I(i, j)$  is the input image;  $F$  and  $F^{-1}$  denote the Fourier transform and inverse Fourier transform respectively;  $A(f)$  is the amplitude spectrum;  $P(f)$  denotes the phase spectrum;  $L(f)$  is the log spectrum, which will be used to calculate the spectrum residual  $R(f)$ .  $h_n(f)$  is a local average filter and the filter size is set to 3 ( $n = 3$ ) in this work.  $g(i, j)$  is a Gaussian smooth filter (the scale factor is set to 8), which can improve the visual effects of output saliency map  $S(i, j)$ .

$$h_n(f) = \begin{pmatrix} 1 & 1 & 1 \\ 1 & 1 & 1 \\ 1 & 1 & 1 \end{pmatrix} / 9 \quad (6)$$

### C. THE RELATIONSHIP OF TOPOLOGICAL PROPERTIES AND SPECTRAL RESIDUAL SALIENCY MAP

The spectral residual approach simulates the pre-attention stage of the human visual system and can find the "pop up" object automatically and quickly. Thus, the saliency map detected by the spectral residual method is consistent with the core idea of topological perception theory.

The content in the saliency map reflects the topological properties perceived in the earlier vision stage. Based on the above analysis, the saliency map calculated by the spectral residual approach is used to express the topological properties in this work.

## III. TOPOLOGICAL PROPERTIES MOTIVATED PCNN

### A. THE CLASSICAL PCNN

The classical PCNN model was proposed by Johnson et al [1] and is successfully used in many image processing fields nowadays. Its fundamental basis is the  $\gamma$  band synchronous spike dynamics of neuronal activity in cat visual cortex. For the neuron  $N_{ij}$  in classical PCNN, the discrete model can be described by the following equations [2].

$$F_{ij}(n) = e^{-\alpha F} F_{ij}(n-1) + V_F \sum_{kl} M_{ijkl} Y_{kl}(n-1) + I_{ij} \quad (7)$$

$$L_{ij}(n) = e^{-\alpha L} L_{ij}(n-1) + V_L \sum_{kl} W_{ijkl} Y_{kl}(n-1) \quad (8)$$

$$U_{ij}(n) = F_{ij}(n)(1 + \beta L_{ij}(n)) \quad (9)$$

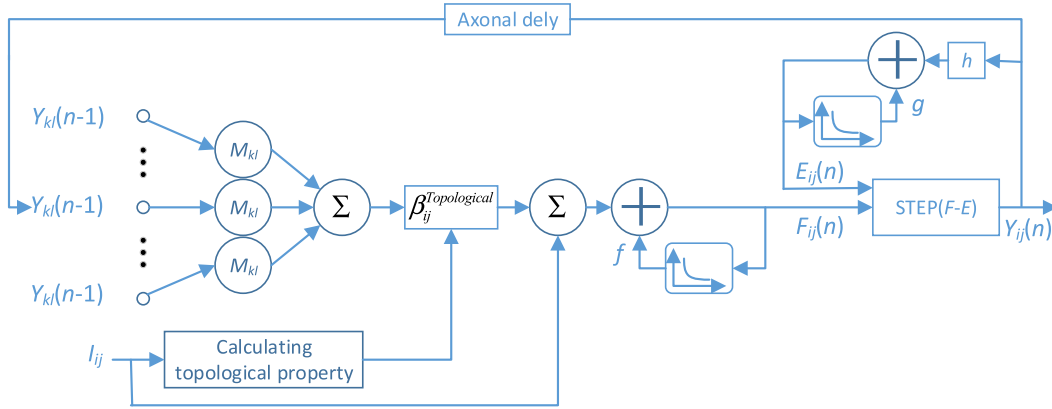


FIGURE 1. The structure of simplified topological based PCNN (TPCNN).

$$Y_{ij}(n) = \begin{cases} 1, & \text{if } U_{ij}(n) > E_{ij}(n-1) \\ 0, & \text{else} \end{cases} \quad (10)$$

$$E_{ij}(n) = e^{-\alpha_E} E_{ij}(n-1) + V_E Y_{ij}(n) \quad (11)$$

where the subscript  $ij$  denotes the position of neuron  $N_{ij}$ ,  $(k, l)$  is one of the neighbor's position of neuron  $N_{ij}$ ;  $F_{i,j}[n]$  and  $L_{i,j}[n]$  denote the feeding input and linking input for neuron  $N_{ij}$  in iteration  $n$ ;  $\alpha_F$ ,  $\alpha_L$  and  $\alpha_E$  are the exponential attenuation time constants of  $F_{i,j}[n]$ ,  $L_{i,j}[n]$  and  $E_{i,j}[n]$  respectively;  $V_F$ ,  $V_L$  and  $V_E$  denote the amplitudes of  $F_{i,j}[n]$ ,  $L_{i,j}[n]$  and  $E_{i,j}[n]$ ;  $M$  and  $W$  are synaptic weight matrices for  $F_{i,j}[n]$  and  $L_{i,j}[n]$ ;  $\beta$  is the linking strength coefficient.

There is a one-to-one correspondence between the positions of neurons and image pixels when the PCNN model is used to process image. The feeding input  $F_{i,j}[n]$  and the linking input  $L_{i,j}[n]$  will be modulated by the linking strength coefficient  $\beta$  to yield internal activity  $U_{i,j}[n]$  when the feeding input receives an input stimulus (such as the normalized gray intensity) through  $I_{ij}$ . Then, the internal activity  $U_{i,j}[n]$  will be compared with the dynamic threshold of the previous iteration  $E_{i,j}[n-1]$  to generate the pulse output  $Y_{i,j}[n]$  of neuron  $N_{ij}$  by equation (10). The dynamic threshold  $E_{i,j}[n]$  will increase suddenly by the amplitude  $V_E$  if the neuron  $N_{ij}$  fires ( $Y_{i,j}[n] = 1$ ). Otherwise, if the neuron  $N_{ij}$  doesn't fire ( $Y_{i,j}[n] = 0$ ), the dynamic threshold  $E_{i,j}[n]$  would decay by coefficient  $e^{-\alpha_E}$  during each iteration until the internal activity  $U_{i,j}[n]$  surpasses the last dynamic threshold  $E_{i,j}[n-1]$  and the neuron  $N_{ij}$  fires again. The output pulse signal  $Y_{i,j}[n]$  is then fed back to the input of the neuron  $N_{ij}$  with a delay of one iteration. A series of pulse images will be outputted by iterating the discrete equations (7) ~ (11).

### B. TOPOLOGICAL PROPERTIES MOTIVATED PCNN

With the wide application of PCNN, many improved simplified PCNN models are proposed, such as SCM [11], SPCNN [12], FLM [6], [14], etc. To reduce the algorithmic complexity and improve the robustness of invariant features calculated by PCNN model, we introduce topological properties into the simplified PCNN model. We call these

topological properties motivated PCNN as TPCNN and the mathematical expressions of TPCNN can be described by formulas (12) ~ (15).

$$F_{ij}(n) = fF_{ij}(n-1) + I_{ij} + \beta_{ij}^{\text{Topological}} \sum_{kl} M_{ijkl} Y_{kl}(n-1) \quad (12)$$

$$Y_{ij}(n) = \begin{cases} 1, & \text{if } F_{ij}(n) \geq E_{ij}(n) \\ 0, & \text{else} \end{cases} \quad (13)$$

$$E_{ij}(n) = gE_{ij}(n-1) + hY_{ij}(n) \quad (14)$$

$$\beta_{ij}^{\text{Topological}} = \xi + \text{Normalize}(|S(i, j)|) \quad (15)$$

where  $f$  and  $g$  are attenuation constants and usually  $f = 0.9$  and  $g = 0.8$ ;  $h$  denotes the amplitudes of  $E_{i,j}[n]$  and usually  $h = 20$ ; To pay close attention to the important targets in the image, when we calculating the invariant features, the topological property coefficient  $\beta_{ij}^{\text{Topological}}$  is adopted as the feeding strength in equation (12);  $S(i, j)$  is the saliency map obtained by the spectral residual approach,  $|\cdot|$  denotes the absolute operate; The  $\text{Normalize}()$  function changes the intensity value of each pixel in the absolute saliency map into the range of 0 to 1;  $\xi$  is a little positive constant to avoid all-zero region in coefficient  $\beta_{ij}^{\text{Topological}}$  and  $\xi$  equals to 0.6 in the following sections. The meanings of other parameters in TPCNN are same as classical PCNN described by equations (7) ~ (11). The structure of TPCNN is displayed in Figure 1.

For an input color image  $I_{ij}$ , a series of binary pulse images  $Y(1); Y(2); \dots; Y(n)$  are outputted when TPCNN is iterated  $n$  times. The image invariant feature usually can be calculated by two methods: time signature [7] and entropy signature [10]. As the entropy is more suitable for measuring the information contained in the output pulse image, the entropy signature is used in the following sections. The entropy used in TPCNN can be expressed by equation (16).

$$H(P) = -P_1 \log_2(P_1) - P_0 \log_2(P_0) \quad (16)$$

where  $H(P)$  denotes the entropy of the output binary image,  $P_1$  and  $P_0$  are the probabilities of 1 and 0 occurred in the

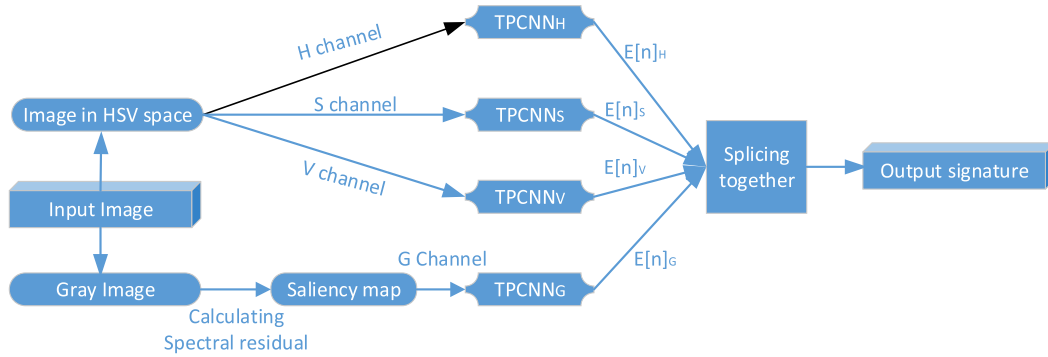


FIGURE 2. Diagram of color image invariant features extraction by TPCNN.

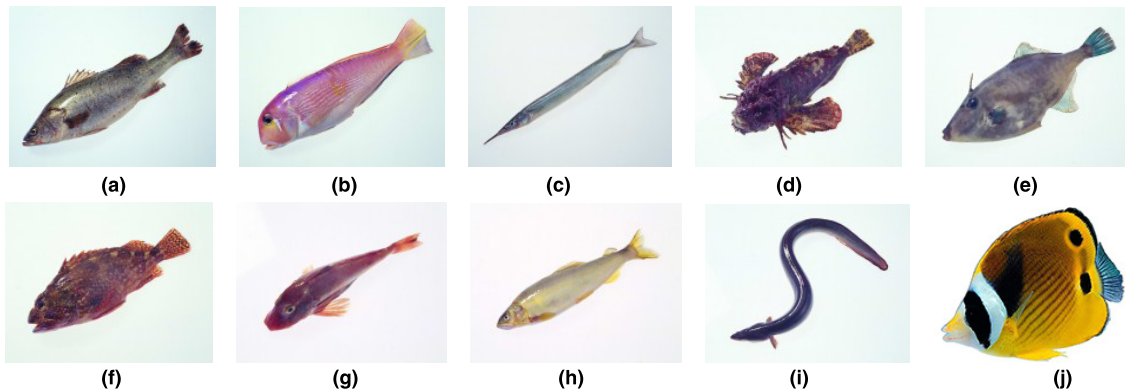


FIGURE 3. Ten species of fish for invariant feature extraction. (a) fish1, (b) fish2, (c) fish3, (d) fish4, (e) fish5, (f) fish6, (g) fish7, (h) fish8, (i) fish9, (j) fish10.

output binary image. The Euclidean distance is selected to evaluate the difference of two image signatures. It is calculated by formula (17).

$$Dist_{12} = \sqrt{\sum_{k=1}^N (E_{1k} - E_{2k})^2} \quad (17)$$

where  $E_{1k}$  and  $E_{2k}$  are two entropy signatures calculated by TPCNN,  $N$  is the length of signature.

#### IV. COLOR IMAGE INVARIANT FEATURES EXTRACTION BY TPCNN

Although RGB color space is widely used many image applications, the relationship of each color component is still unclear and they are not suitable for the human vision system to understand. Based on this fact, the input color image is transformed from RGB color space to HSV color space firstly. After that, the signatures of H channel, S channel and V channel are computed by TPCNN. On the other side, the input color image is changed to a gray image for extracting topological properties by the spectral residual approach. The topological properties, denoted as G channel in Figure 2, will be used as the linking strength in TPCNN model and to computing the topological invariant feature by TPCNN. In the end, the signatures computed from four channels are

spliced together and the final color image invariant features are obtained. The diagram of above computing process is shown in Figure 2.

#### V. EXPERIMENTS AND ANALYSIS

In our view, a good image signature should have good distinguishability and strong robustness. For the distinguishability, the Euclidean distance calculated by formula (17) is used as a quantitative evaluation criteria. The Euclidean distance between different types of targets is bigger the distinguishability of the signature is better. For the robustness, the variations of the Euclidean distances of the same target under different transformations (such as rotation, zooming in and out etc.) are smaller the robustness of the signatures are stronger. To give a visual and quantitative evaluation about the signature calculated by TPCNN model, the distinguishability and robustness of the signatures obtained by TPCNN are compared with classical PCNN and other familiar simplified PCNN models such as SPCNN, SCM, and FLM. The test results of ten species of fish's color images (displayed in Figure 3) are listed in the following sub-sections.

The initial values of  $F$ ,  $Y$ , and  $E$  in TPCNN are zeros. The other parameters are set as following:  $f = 0.9$ ;  $h = 20$ ;  $g = 0.8$ ;  $W = [0.1091 \ 0.1409 \ 0.1091; 0.1409 \ 0 \ 0.1409; 0.1091 \ 0.1409 \ 0.1091]$ ; Iteration number  $N = 30$ .

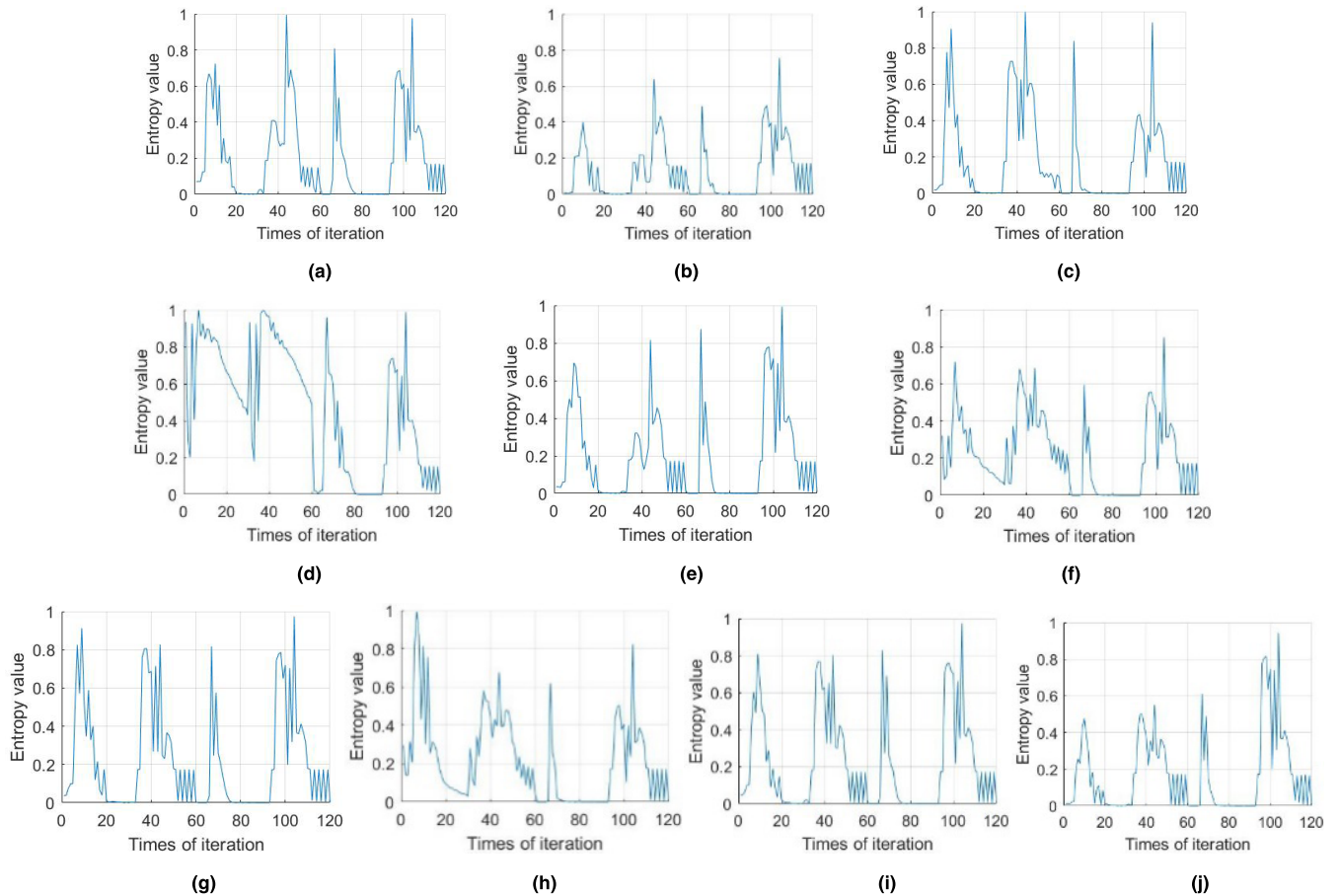


**FIGURE 4.** Signatures of ten species fish in Fig.3 calculated by TPCNN. (a) fish1, (b) fish2, (c) fish3, (d) fish4, (e) fish5, (f) fish6, (g) fish7, (h) fish8, (i) fish9, (j) fish10.

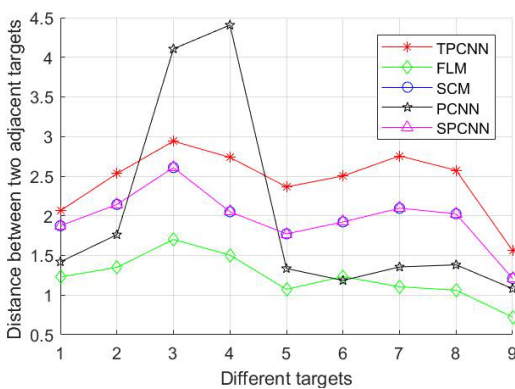


**FIGURE 5.** Distance curves of adjacent targets with different algorithms.

**A. COLOR IMAGES OF TEN SPECIES FISH AND THEIR SIGNATURE CURVES**

The entropy signature curves of ten species fish, calculated by TPCNN, are plotted in Figure 4. Obviously, the visual appearance shapes of the signature’s curves are different. To give a quantitative evaluation of the distinguishability about the TPCNN signature, the Euclidean distance curves between two different species fish are given in Figure 5. Table 1 listed

the variations of the signatures under different transformation and the robustness of the TPCNN is proved too.

**B. DISTINGUISHABILITY CURVES BETWEEN SIGNATURES OF DIFFERENT SPECIES FISH**

In order to verify the distinguishability of the TPCNN signature, we compared TPCNN with classical PCNN, SPCNN, SCM, and FLM. We calculate the signatures’ distances between ten species fish using the above five neural network models. The distinguishability curves are plotted in Figure 5. The distinguishability curve of TPCNN is plotted by a red color solid line and the signature distances of the ten species fish are varying from 1.6 to 3. The distinguishability curves of the classical PCNN, SPCNN, SCM, and FLM are plotted by a black line, a pink line, a blue line and a green line respectively.

The results show that the distinguishability of the classical PCNN is better than TPCNN only at two points and inferior to TPCNN at other seven points. The overall performance of TPCNN is outperformed than classical PCNN. The performance of SCM is almost the same as SPCNN and their distinguishability curves are completely overlap. The distinguishability of FLM is lowest. Through the above comparison, we know that the distinguishability of the TPCNN has the best performance.

**TABLE 1. The variance of TPCNN signature under different transformation.**

|        | Rotate<br>90 degrees | Rotate<br>180 degrees | Rotate<br>270 degrees | Shrink<br>0.7 times | Shrink<br>0.8 times | Shrink<br>0.9 times | Magnify<br>1.1 times | Magnify<br>1.2 times | Magnify<br>1.3 times |
|--------|----------------------|-----------------------|-----------------------|---------------------|---------------------|---------------------|----------------------|----------------------|----------------------|
| Fish1  | 0.2503               | 0.2152                | 0.2867                | 0.1371              | 0.0852              | 0.0937              | 0.0791               | 0.0985               | 0.0819               |
| Fish2  | 0.3591               | 0.1679                | 0.4233                | 0.1499              | 0.0882              | 0.0826              | 0.0692               | 0.0743               | 0.0481               |
| Fish3  | 0.1923               | 0.1496                | 0.1832                | 0.1645              | 0.0905              | 0.1130              | 0.0816               | 0.1144               | 0.0673               |
| Fish4  | 0.2556               | 0.2303                | 0.2536                | 0.2732              | 0.2254              | 0.2101              | 0.1714               | 0.1775               | 0.1637               |
| Fish5  | 0.5804               | 0.1401                | 0.5905                | 0.1666              | 0.1296              | 0.0869              | 0.1163               | 0.0733               | 0.0924               |
| Fish6  | 0.2430               | 0.0887                | 0.2279                | 0.2080              | 0.1263              | 0.1027              | 0.0856               | 0.1092               | 0.0902               |
| Fish7  | 0.1681               | 0.1533                | 0.2057                | 0.1725              | 0.0949              | 0.0783              | 0.0593               | 0.0869               | 0.0804               |
| Fish8  | 0.6007               | 0.1594                | 0.6065                | 0.2484              | 0.1837              | 0.1704              | 0.1490               | 0.1731               | 0.1698               |
| Fish9  | 0.1798               | 0.1385                | 0.2460                | 0.1704              | 0.1038              | 0.0771              | 0.0626               | 0.0953               | 0.0939               |
| Fish10 | 0.5526               | 0.1592                | 0.5163                | 0.2026              | 0.1131              | 0.1041              | 0.0645               | 0.1111               | 0.0763               |

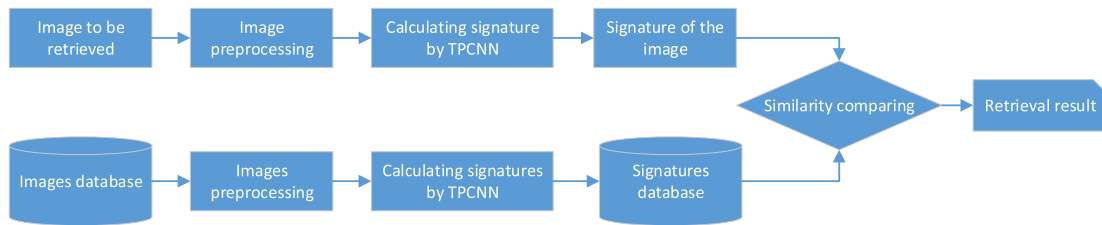


**FIGURE 6. Structure of the CBIR system based on TPCNN signature.**

**C. ROBUSTNESS BETWEEN DIFFERENT TRANSFORMATIONS**

To test the robustness of the TPCNN signature, we rotate the targets of ten species fish with different angles and magnify the targets with different factors. Table 1 lists the typical Euclidean distances variations about the ten species fish under different transformations. The test results shown that the signature distance of each fish varies very small. In other words, the signature calculated by TPCNN has strong robustness.

**VI. APPLICATIONS OF COLOR IMAGE INVARIANT FEATURES EXTRACTED BY TPCNN**

The invariant features extracted by TPCNN can be used in many image processing fields, such as content-based image retrieval, specific target identification and detection, image authentication and tampering area detection, etc.

**A. CONTENT BASED IMAGE RETRIEVAL**

In general, content-based image retrieval (CBIR) [20], [21] is using image content features to retrieve images from a large image database or the Internet. The core technique of CBIR is how to extract the image invariant feature effectively. It is known that PCNN is inspired by the working principle of the mammalian visual nervous system. Thus PCNN has many inherent superiorities than other models when it is used to extract image features. The structure of a CBIR system based on TPCNN signature is displayed in Figure 6.

Firstly, we should construct a large image signatures database by the offline calculating method. All the images should have a preprocessing stage, some operations such as:

to normalize image size, adjust image brightness, etc. can be adopted in this stage. The signatures of the images should be calculated after the preprocessing stage. The signatures database can be constructed by repeat the prior operation in offline mode.

When we retrieval an image from the image database, the TPCNN signature of the image should be calculated in an online method. Finally, we can use the specific image signature to compare in the signature database. A certain number of the result images will be obtained and the images will be sorted by similarity.

**B. SPECIFIC TARGET IDENTIFICATION**

The structure of the specific target identification system based on TPCNN signature is basically the same as CBIR system displayed in figure 6.

The main difference between the two systems is that the signatures in specific target identification system are specific targets' signatures instead of the whole image's signature. For the case of multiple targets in an image, we should adopt other segmentation algorithms to extract out the target firstly. The other processing steps in specific target identification system are the same as a content-based image retrieval system.

**C. IMAGE AUTHENTICATION AND TAMPERING AREA DETECTION**

With the development of information technology, digital images can be easily modified by many image processing software. Thus, more and more attention has been paid to the image authentication technology in recent years. In brief, image authentication is one kind of technology to

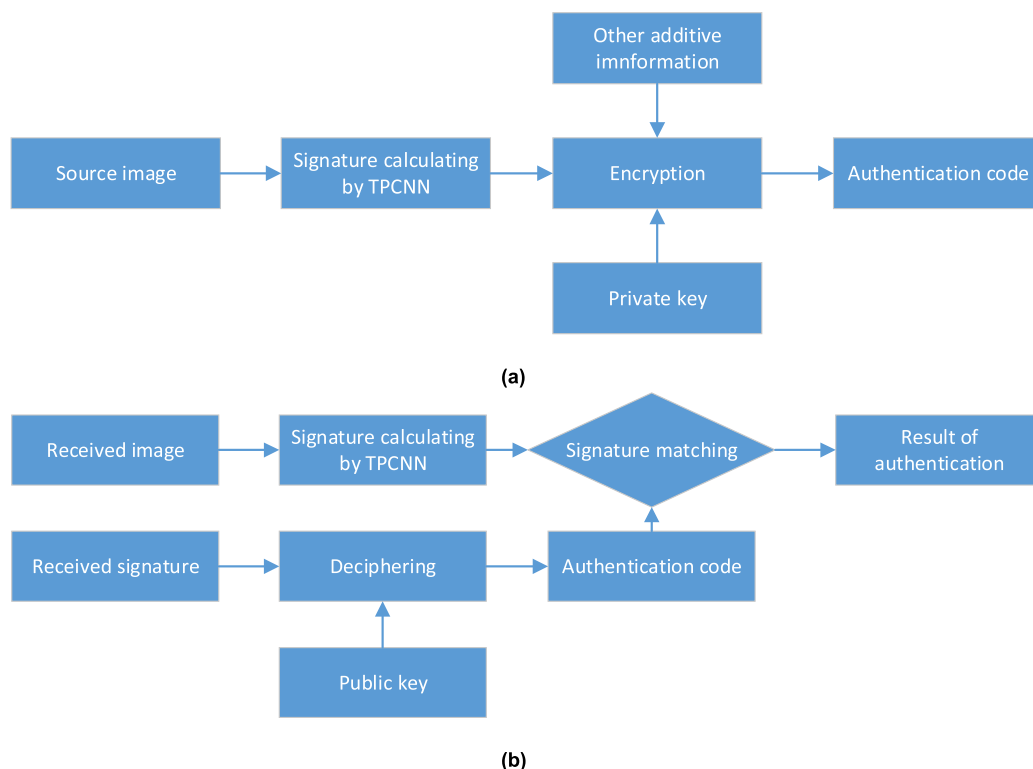


**FIGURE 7.** Diagram of the image authentication system based on TPCNN signature. (a) Source side. (b) Receiving side.

protect the image integrity from illegally modified [7], [22]. There are two categories of image authentication schemes: signature-based schemes and watermark-based schemes. Feature extraction plays an important role in signature-based schemes. The ordinary feature extraction approaches include hash function, local histogram, and local mean intensity, etc. All the signature-based authentication schemes do not need to embed any information into the original image that is the watermark-based schemes must do. Better performance can be obtained if the signature calculated by TPCNN is used to the authentication systems, as this kind of signature has many advantages, such as translation, rotation, and scale invariance. The diagram of image authentication system based on TPCNN signature is displayed in Figure 7.

To detect the tampering area in the image, we can divide the original image and the received image to  $n$  sub-blocks in the same way and calculate their signatures independently. Then, the sub-block number of the tampering area can be located by comparing the corresponding signatures. In the practical application, we should have a compromise between the sub-blocks number and the location accuracy of the tampering areas. In other words, the more image sub-blocks we divided (the more authentication data needed), the more location accuracy of the tampering areas we can obtain.

## VII. CONCLUSION

By analyzing the topological perception theory, the spectral residual approach is used to extract the topological properties. After introducing the topological properties into the

simplified PCNN model, a topological property based simplified PCNN (TPCNN) is proposed. The TPCNN model is successfully used to extracting the color image invariant features. The signature calculated by TPCNN has many advantages, such as high computing efficiency, invariance with translation, rotation and scale changing. The experiment results have proven the robustness and effectiveness of the signature calculated by TPCNN. Some common applications of the signature are discussed in the work too.

## REFERENCES

- [1] J. L. Johnson and M. L. Padgett, "PCNN models and applications," *IEEE Trans. Neural Netw.*, vol. 10, no. 3, pp. 480–498, May 1999.
- [2] G. Kuntimad and H. S. Ranganath, "Perfect image segmentation using pulse coupled neural networks," *IEEE Trans. Neural Netw.*, vol. 10, no. 3, pp. 591–598, May 1999.
- [3] Z. Yang, J. Lian, Y. Guo, S. Li, D. Wang, W. Sun, and Y. Ma, "An overview of PCNN model's development and its application in image processing," *Arch. Comput. Methods Eng.*, vol. 26, no. 2, pp. 491–505, Apr. 2019.
- [4] C. Wu, Z. Liu, and H. Jiang, "Catenary image segmentation using the simplified PCNN with adaptive parameters," *Optik*, vol. 157, pp. 914–923, Mar. 2018.
- [5] Z. Yang, J. Lian, S. Li, Y. Guo, Y. Qi, and Y. Ma, "Heterogeneous SPCNN and its application in image segmentation," *Neurocomputing*, vol. 285, pp. 196–203, Apr. 2018.
- [6] K. Zhan, J. Teng, J. Shi, and M. Wang, "Feature-Linking model for image enhancement," *Neural Comput.*, vol. 28, no. 6, pp. 1072–1100, Jun. 2017.
- [7] G. Kou, Y. Ma, and J. Yue, "A bio-inspired authentication approach to colour image transmitted on open non-secure public network," *Int. J. Commun. Netw. Distrib. Syst.*, vol. 18, no. 2, pp. 148–161, Jan. 2017.
- [8] X. Gu, "Feature extraction using unit-linking pulse coupled neural network and its applications," *Neural Process. Lett.*, vol. 27, no. 1, pp. 25–41, Feb. 2008.

- [9] W. Huang and Z. Jing, "Multi-focus image fusion using pulse coupled neural network," *Pattern Recognit. Lett.*, vol. 28, no. 9, pp. 1123–1132, 2007.
- [10] G. J. Kou, J. Yue, and Y. Y. Ma, "SAR image invariant feature extraction by anisotropic diffusion and multi-gray level simplified PCNN," *IEEE Access*, vol. 7, pp. 47135–47142, 2019.
- [11] K. Zhan, H. Zhang, and Y. Ma, "New spiking cortical model for invariant texture retrieval and image processing," *IEEE Trans. Neural Netw.*, vol. 20, no. 12, pp. 1980–1986, Dec. 2009.
- [12] Y. Chen, Y. Ma, D. H. Kim, and S.-K. Park, "Region-based object recognition by color segmentation using a simplified PCNN," *IEEE Trans. Neural Netw. Learn. Syst.*, vol. 26, no. 8, pp. 1682–1697, Aug. 2015.
- [13] K. Zhan, J. Teng, and Y. Ma, "Spiking cortical model for rotation and scale invariant texture retrieval," *J. Inf. Hiding Multimedia Signal Process.*, vol. 4, pp. 155–165, Jul. 2013.
- [14] K. Zhan, J. Shi, H. Wang, Y. Xie, and Q. Li, "Computational mechanisms of pulse-coupled neural networks: A comprehensive review," *Arch. Comput. Methods Eng.*, vol. 24, pp. 573–588, Jul. 2017.
- [15] L. Chen, "Topological structure in visual perception," *Science*, vol. 218, no. 4573, pp. 699–700, Nov. 1982.
- [16] L. Chen, "The topological approach to perceptual organization," *Vis. Cognit.*, vol. 12, no. 4, pp. 553–637, 2005.
- [17] X. Hou and L. Zhang, "Saliency detection: A spectral residual approach," in *Proc. IEEE Conf. Comput. Vis. Pattern Recognit.*, Jul. 2007, pp. 1–9.
- [18] X. Gu, Y. Fang, and Y. Wang, "Attention selection using global topological properties based on pulse coupled neural network," *Comput. Vis. Image Understand.*, vol. 117, no. 10, pp. 1400–1411, Oct. 2013.
- [19] Y. Zhang, F. Zhang, and L. Guo, "Saliency detection by selective color features," *Neurocomputing*, vol. 203, pp. 34–40, Aug. 2016.
- [20] R. R. Saritha, V. Paul, and P. G. Kumar, "Content based image retrieval using deep learning process," *Cluster Comput.*, vol. 1, pp. 1–14, Feb. 2018.
- [21] M. M. Mohammed, A. Badr, and M. B. Abdelhalim, "Image classification and retrieval using optimized pulse-coupled neural network," *Expert Syst. Appl.*, vol. 42, no. 11, pp. 4927–4936, Jul. 2015.
- [22] C.-C. Lo and Y.-C. Hu, "A novel reversible image authentication scheme for digital images," *Signal Process.*, vol. 98, pp. 174–185, May 2014.



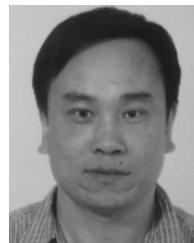
**GUANGJIE KOU** received the B.S. and M.S. degrees in computer science and technology from Qufu Normal University, in 2000 and 2003, respectively, and the Ph.D. degree in computer science and technology from the Institute of Computing Technology, Chinese Academy of Sciences (CAS), Beijing, China, in 2011. He is currently an Associate Professor with the School of Information and Electrical Engineering, Ludong University, Yantai, China. His research interests include digital image processing and computer vision.



**JUN YUE** received the Ph.D. degree in management science and engineering from China Agricultural University, Beijing, China. She is currently a Professor with the School of Information and Electrical Engineering, Ludong University, Yantai, China. Her research interests include computer vision and deep learning.



**YUNYAN MA** received the B.S. and M.S. degrees in probability theory and mathematical statistics from Qufu Normal University, in 2000 and 2003, respectively, and the Ph.D. degree in financial mathematics from Shandong University, Jinan, China, in 2012. She is currently a Lecturer with the School of Mathematics and Statistics, Ludong University, Yantai, China. Her research interests include statistical learning and time series analysis.



**ZHIWANG ZHANG** received the Ph.D. degree in computer science from the Chinese Academy of Sciences, in 2009. He is currently a Researcher and an Associate Professor with the School of Information and Electrical Engineering, Ludong University, Yantai, China. He has published over 30 academic papers in various international journals and conferences. His research interests are in the areas of data mining and knowledge discovery, forecasting, machine learning, optimization, artificial intelligence, and natural language processing.

• • •